

Conjugated ethynylene-fluorene polymers with electro-donating TTF as pendant groups: Synthesis, electrochemical and spectroscopic properties

Xuechao Zhang,^a Chengyun Wang,^{*a} Guoqiao Lai,^b Lei Zhang^a and Yongjia Shen^{*a}

Received (in Montpellier, France) 29th September 2009, Accepted 13th November 2009

First published as an Advance Article on the web 8th December 2009

DOI: 10.1039/b9nj00520j

A series of conjugated ethynylene-fluorene polymers with electro-donating **TTF** as pendant groups (**P2–P4**) were synthesized by using Sonogashira coupling reaction, and two functionalization methods, *i.e.* prepolymerization and postpolymerization, were developed. The composition and purity of the corresponding products were analyzed by ¹H NMR. The results proved the functionalization of **P2** (pre) and **P2** (post) were 40% and 100%, respectively. The results also indicated that the postpolymerization method would be a better approach to prepare **TTF**-pendant conjugated ethynylene-fluorene polymers. The postpolymerization methodology could be extended to synthesize other conjugated fluorene-based polymers bearing **TTF** units (**P3** and **P4**). The polymers mentioned above exhibited good solubility in normal organic solvents and higher conductivity (neutral conductivity $\sim 2\text{--}4 \times 10^{-6} \text{ S cm}^{-1}$; doped conductivity $\sim 1\text{--}3 \times 10^{-3} \text{ S cm}^{-1}$). Moreover, the fluorescence intensity of **P2** (post) could be modulated by the oxidation of **TTF** units, which makes it an attractive candidate for the fluorescence switch.

Introduction

Tetrathiafulvalene (**TTF**) and its derivatives have attracted a great deal of attention over the last four decades since they were strong electron donors and could be oxidized and reduced reversibly.¹ With this unique feature, molecules containing **TTF** units have been used in many fields,² such as organic metals,³ molecular logic gates,⁴ and molecular sensors.^{5,6} In recent years, the **TTF** and their derivatives have been incorporated into conjugated polymers,⁷ for example, polythiophenes,^{8,9} polycarbazole¹⁰ and polysilanes.¹¹ The concept of merging **TTF** units with linear conjugated polymers offers exciting potential to develop novel conducting polymers.¹² From the viewpoint of **TTF** chemistry, such a combination may improve the conductivity of the **TTF**-polymer based conductors, due to increasing dimensionality of the conductors in their solid state.^{7,13}

In the past decade, studies have shown that fluorene-based materials hold great potential applications, such as light-emitting materials,^{14–16} and nonlinear optical materials.¹⁷ In our previous research,¹⁸ oligofluorenes with pendant **TTF** units have found their use in conducting material and fluorescence switch. Recently, the conjugated fluorene polymers with ethynyl units in the backbone have drawn great attention, due to their excellent electrochemical and spectroscopic properties together with their facile substitution at the C₉ site, which provides the possibility of introducing new

functional units to the backbone.¹⁹ The acetylene linkages can enhance the planarity and induce stronger intermolecular interactions among the chromophores. This π – π stacking between aromatic chromophores can lead to higher charge transportation. In this regard, the incorporation of the electro-donating **TTF** units with conjugated polymers with ethynyl units in the backbone would be a convenient method to obtain new functional materials, namely, **TTF**-carried fluorene-ethynylene polymers. As a matter of fact, the examples of the attachment of **TTF** to the conjugated fluorene backbone are still limited.^{13,20} Moreover, in comparison to single or double bond linked fluorene polymers, triple bond linked fluorene polymers are not abundantly reported.^{21,22}

In this article, we synthesized and characterized a series of conjugated **TTF**-carried ethynylene-fluorene polymers by using a sonogashira coupling method, in order to study the effects of **TTF** units on electrochemical and spectroscopic properties of the ethynylene-fluorene backbone. These polymers exhibited good solubility and higher conductivity. Moreover, the fluorescence intensity of these polymers could be modulated by the oxidation of **TTF** units, which makes them attracting candidates of the fluorescence switches.

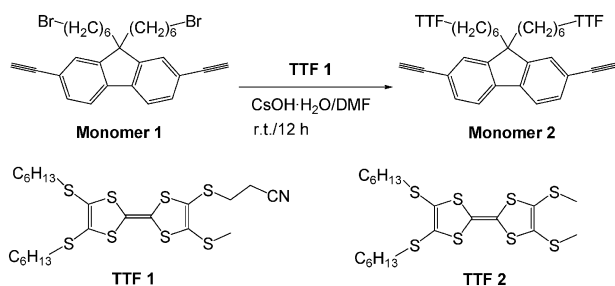
Results and discussion

Synthesis and characterization of the polymers

We conducted postpolymerization and prepolymerization functionalization approaches to prepare **TTF**-bearing conjugated fluorene copolymers by using sonogashira coupling reaction.²³ In the case of postpolymerization, cyano-ethyl groups in **TTF** **1**^{24,25} was deprotected by CsOH·H₂O to afford **TTF** thiolates and then trapped by **Monomer 1** to form **Monomer 2** (Scheme 1). Copolymerization of **Monomer 2** and

^a Key Laboratory for Advanced Materials and Institute of Fine Chemicals, East China University of Science & Technology, Shanghai 200237, P. R. China. E-mail: yjshen@ecust.edu.cn, cywang@ecust.edu.cn

^b Key Lab of Organosilicon Chemistry and Material Technology of Ministry of Education, Hangzhou Normal University, Hangzhou 310012, P. R. China



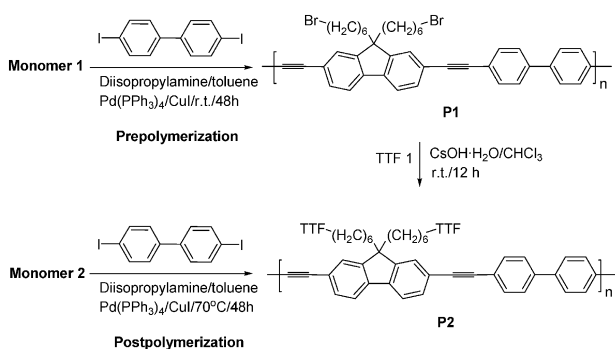
Scheme 1 Synthetic route to **Monomer 2** and the structure of compound **TTF 1** and **TTF 2**.

4,4'-diiodobiphenyl gave **P2** (post) as a brown solid through the sonogashira coupling polymerization (Scheme 2). In the case of prepolymerization, the fluorene-based conjugated polymer (**P1**) with leaving bromide groups was obtained. Both **TTF**-carried and fluorene-based conjugated polymer **P2** (pre) were obtained by the reaction of **P1** and **TTF** caesium salt, which was synthesized by deprotecting cyanoethyl groups in **TTF 1** in the presence of one equivalent of caesium hydroxide monohydrate ($\text{CsOH} \cdot \text{H}_2\text{O}$).

^1H NMR analysis of the products showed that there were no Br atoms in **P2** (post), while some Br atoms in **P2** (pre) were detected, which means they were not completely reacted with **TTF** caesium salt. The ratios of the numbers of H atoms belonging to $\text{Br}-\text{CH}_2$ and $\text{S}-\text{CH}_2$ plus $\text{S}-\text{CH}_3$ proved the functionalization of **P2** (pre) and **P2** (post) were 40% and 100% (Fig. 1), respectively. The low functionalization of the **P2** (pre) might be ascribed to the steric hindrance effect of the **TTF** unit which linked to the fluorene backbone.

The prepolymerization and postpolymerization methodologies of synthesizing **P2** could be extended to synthesize other conjugated fluorene-based polymers bearing **TTF** units. Thus, another two polymers were synthesized by reacting 4,4'-diiodobiphenyl ether (**P3**) and 2,5-diiodoxyline (**P4**) instead of 4,4'-diiodobiphenyl, using the postpolymerization method (Scheme 3).

For comparison, **P5** without **TTF** units was also synthesized by reaction **Monomer 3** and 4,4'-diiodobiphenyl in a similar way (yield 50.2%). The formed conjugated fluorene-based polymers bearing electro-donating **TTF** as pendant groups are soluble in common solvents, such as, chloroform dichloromethane and THF.



Scheme 2 Synthetic route to **P2** using prepolymerization and postpolymerization functionalization methods.

Electrochemistry

The redox properties of **P2–P4** were studied by cyclic voltammetry (CV) in CH_2Cl_2 and their CV curves were presented in Fig. 2. The electrochemical behavior of the model polymer **P5** was also investigated under the similar conditions. For comparison, the electrochemical data of model **TTF 2** were listed in Table 1 as well.

CV curves of **P2–P4** showed two single-electron reversible redox processes, corresponding to the successive generation of the radical cation $\text{TTF}^{+\bullet}$ and dication TTF^{2+} ($E_{\text{ox1}}^{1/2}$ and $E_{\text{ox2}}^{1/2}$) respectively.¹⁰ While, these two processes were followed by two irreversible oxidation processes ($E_{\text{ox1}}^{\text{flu}}$ and $E_{\text{ox2}}^{\text{flu}}$). For the **TTF** units in **P2** (pre), there was about 10 mV cathodic shift related to the first redox potential and no change related to the second redox potential, compared with **TTF 2**, suggesting that the attachment of **TTF** units to the polyfluorene in **P2** (pre) cause a slight effect on the fluorene backbone. The small cathodic shift could be ascribed to the electronic or steric effect between them. Similarly, the polymer **P2** (post) obtained by using the postpolymerization method, revealed the same potential (0.50 V) in the first redox process. However, the increasing amount (40% to 100%) of the **TTF** unit in each repeat unit caused another cathodic shift (0.86 V to 0.84 V) in the second redox process, because the increasing electrostatic repulsion effect between the two $\text{TTF}^{+\bullet}$ moieties, after the first oxidation process (**TTF** to $\text{TTF}^{+\bullet}$). The pendant $\text{TTF}^{+\bullet}$ groups were distorted in order to avoid the involved electric charge crowdedness, facilitating the loss of the electrons.

Compared to the model polymer **P5**, **P2** (post) revealed the emergence of an additional anodic wave around 1.81 V, indicating that the attached **TTF** groups exerted electronic or steric effect on the fluorene backbone. Nevertheless, the additional wave on the CV curve of **P2** (pre) could not be observed obviously. This result could also be attributed to the increasing amount of **TTF** in **P2** (post). As the alkyl chains containing **TTF** units were substituted in the same position of the fluorene and this might cause the stereospecific blockade between the two **TTF** moieties, the fluorene framework would twist and the electron could be lost easily as the descent strength of delocalization pathway of the π -electron system. As a result, the increasing amount of **TTF** groups enhanced this steric effect and the electron in the fluorene backbone lost easily.

The electrochemical behaviors of **P3** and **P4** were similar to that of **P2** (post) and the potentials were nearly the same as **P2** (post). This result indicated that the backbone of the polymers gave a slight effect on the electrochemical properties of the **TTF** attached conjugated polymers and the electro-donating **TTF** made the main contribution to the electronic and steric effect.

UV-Vis spectra

The UV-Vis absorption spectra of **P2–P4** and the models **TTF 2** and **P5** in CH_2Cl_2 were given in Fig. 3.

All the spectra of the polymers have one absorption peak at 227 nm in the ultraviolet region, which could be assigned to the absorption of the long alkyl chains.²⁶ In comparison with the absorption spectrum of the model polymer **P5**, a new

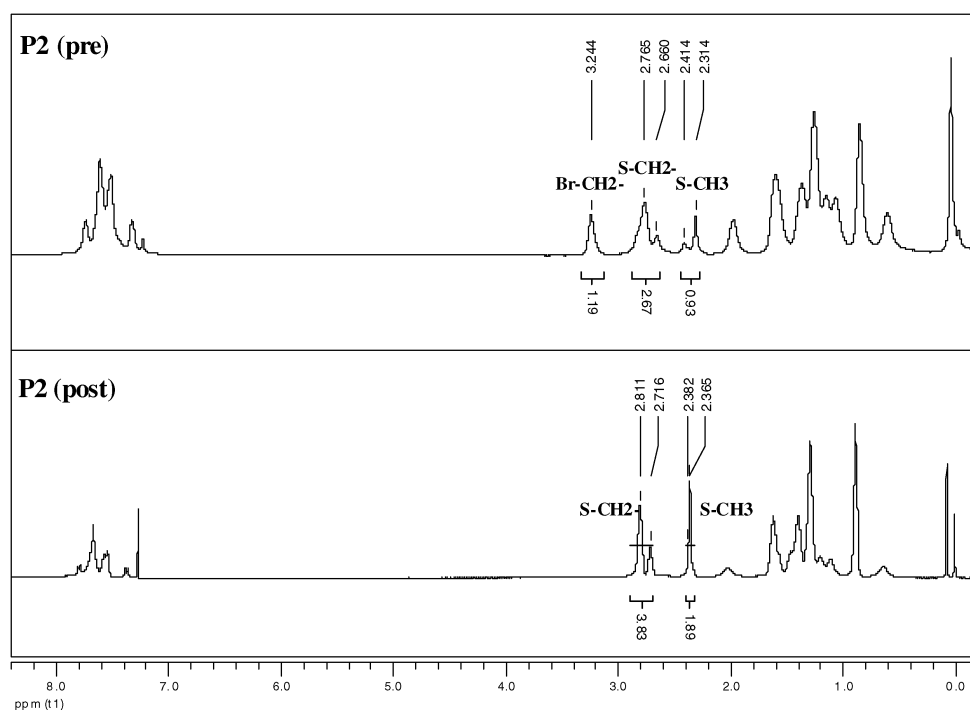
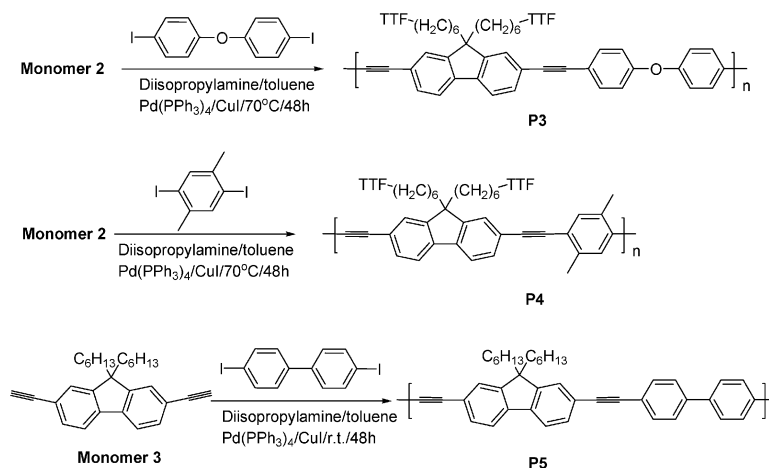


Fig. 1 ^1H NMR spectra of **P2** (pre) and **P2** (post) in CDCl_3 solution.



Scheme 3 Synthetic route to fluorene-based polymers bearing **TTF** pendants (**P3**, **P4**) and the structure of model polymer **P5**.

broad absorption in the region (420–500 nm) emerged and the absorption peak at about 366 nm became bathochromically shifted by about 7–23 nm for the polymers **P2–P4** with pendant **TTF** groups. Clearly the intramolecular charge transfer between the electron-deficient moiety ethynylfluorene and electron-rich moiety **TTF** units exerted bathochromic effect on the electronic transitions of **P2–P4**.²⁷ More evidence for the conclusion could be found in the spectrum of **P2** (pre) and **P2** (post) obtained by using prepolymerization and postpolymerization methods. The absorption curve of **P2** (post) was nearly identical with **P2** (pre) in shape, but the two strong absorption peaks were at 227 nm and 389 nm and a shoulder peak was at 320 nm, *i.e.*, there was a red shift of 16–41 nm compared to **P2** (pre). This red shift indicated an increasing electronic interaction between the conjugated

fluorene main chain and pendant **TTF** units. Obviously, the increasing amount (40% to 100%) of the **TTF** units in each repeat unit could be the main contribution to this red shift, resulting from increasing intramolecular charge transfer interaction between the pendant **TTF** units and fluorene backbone (also see the CV curves above).

Fluorescence spectra

The fluorescence spectra of **P2–P4** containing pendant **TTF** groups were excited at $\lambda_{\text{ex}} = 389$ nm, as shown in Fig. 4. For comparison, the fluorescent spectrum of **P5** is also given in Fig. 4.

As shown in Fig. 4, the fluorescent spectra of **P2** and **P5** were very similar in shape and their spectra with the maximum

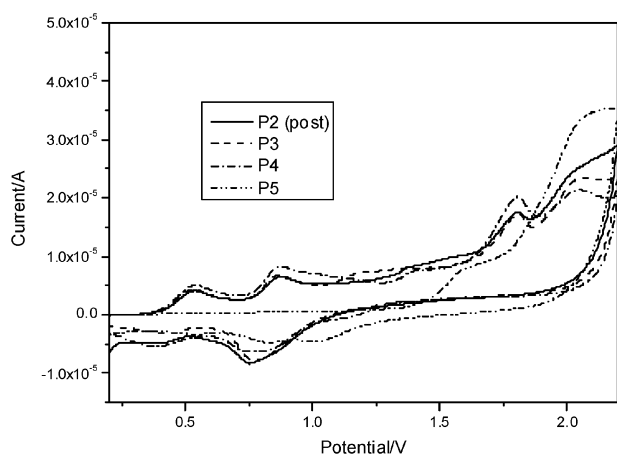


Fig. 2 The cyclic voltammograms of **P2–P5** (1×10^{-3} M) in CH_2Cl_2 (scanning rate 50 mV S^{-1}); platinum as the working and counter electrodes, saturated calomel electrode (SCE) as the reference electrode, $n\text{-Bu}_4\text{NPF}_6$ (0.1 M) as the supporting electrolyte.

Table 1 The electrochemical data of **P2–P5** and **TTF2** in CH_2Cl_2

Compound	$E_{\text{ox1}}^{1/2}/\text{V}$	$E_{\text{ox2}}^{1/2}/\text{V}$	$E_{\text{ox1}}^{\text{flu}}/\text{V}$	$E_{\text{ox2}}^{\text{flu}}/\text{V}$
P2 (pre)	0.50	0.86	2.20	
P2 (post)	0.50	0.84	1.81	2.20
P3	0.49	0.84	1.81	2.20
P4	0.49	0.83	1.81	2.20
P5			2.17	
TTF 2	0.51	0.86		
Monomer 2	0.50	0.84	1.84	2.11

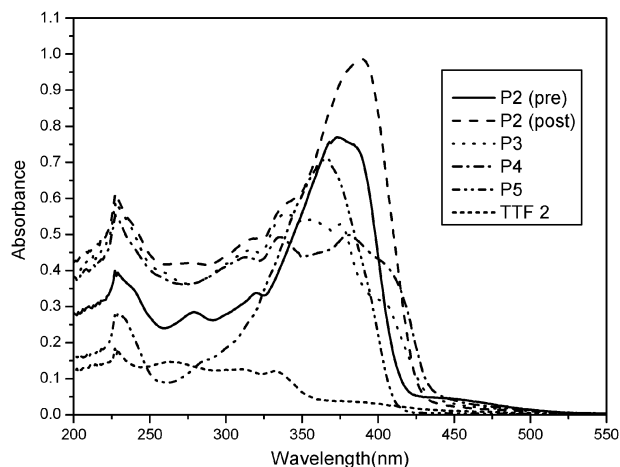


Fig. 3 The absorption spectra of **P2–P5** and **TTF 2** (1×10^{-5} M) in CH_2Cl_2 .

emission peak at around 411 nm were indeed the mirror images of UV/Vis absorption spectrum of the model polymer **P5** (see Fig. 3), indicating that the conjugated fluorene backbone of **P2** made the main contribution to the fluorescence.²⁸ Comparing with the model polymer **P5**, a strong fluorescence quench (*ca.* 99%) was observed for **P2** (post). Perhaps the photo-induced electron transfer (PET) interaction from **TTF** units to the fluorene unit in the excited state was the reason for such fluorescence quench.²⁸ Moreover, **P2** (post) indicated a weaker fluorescence emission than **P2** (pre), indicating an

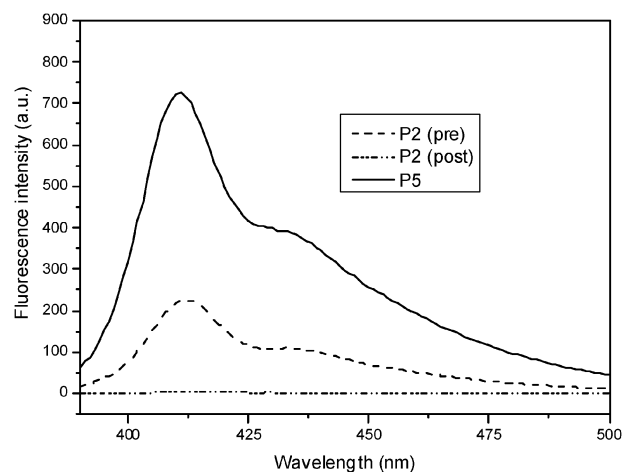


Fig. 4 The fluorescent spectra of **P2–P5** (1×10^{-5} M) in CH_2Cl_2 . $\lambda_{\text{ex}} = 389 \text{ nm}$.

increasing PET interaction between the conjugated fluorene backbone and pendant **TTF** units, due to the increasing amount (40% to 100%) of the **TTF** units in each repeat unit (also see the CV and UV/Vis above). The fluorescent spectra of **P3** and **P4** were similar to that of **P2** (post) and the strong fluorescence quench (*ca.* 99%) were also observed. The PET interaction between the conjugated fluorene backbone and pendant **TTF** units, were slightly influenced by the backbone of the polymers.

Chemical oxidation

The chemical oxidation was carried out in the solution of **P2** (post) in THF by adding increasing amounts of $\text{Fe}(\text{ClO}_4)_3$ to it, in order to examine the potential of **P2** (post) being used as fluorescence switches. The absorption spectra were measured and recorded in Fig. 5.

A new broad absorption band centered at 620 nm emerged on the new absorption spectra after adding $\text{Fe}(\text{ClO}_4)_3$, which could be ascribed to the absorption bands of the **TTF** radical cation.²⁹ Meanwhile, the absorbance at 389 nm decreased with the increasing amount of $\text{Fe}(\text{ClO}_4)_3$ and this could also be

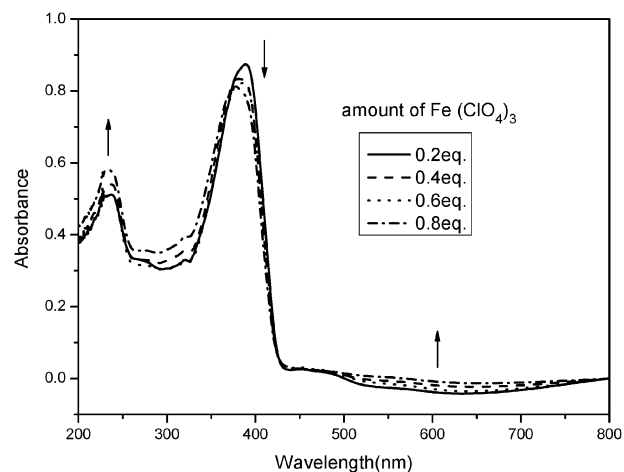


Fig. 5 The absorption spectra of **P2** (post, 1×10^{-5} M) in THF upon addition of increasing amount of the oxidant $\text{Fe}(\text{ClO}_4)_3$.

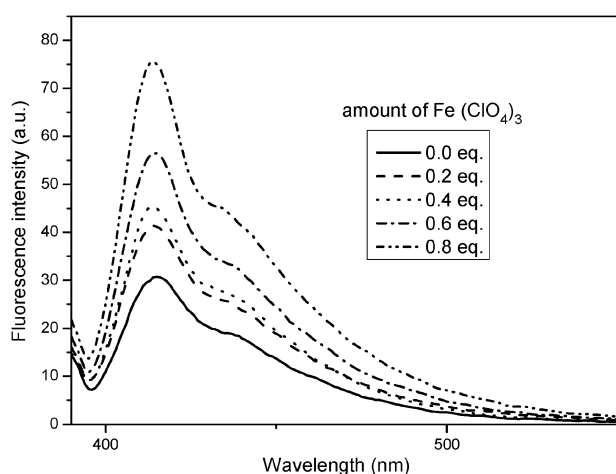


Fig. 6 The fluorescence spectra of **P2** (post, 1×10^{-5} M) in THF upon addition of increasing amount of the oxidant $\text{Fe}(\text{ClO}_4)_3$. $\lambda_{\text{ex}} = 389$ nm.

explained by the same mechanism. This observation implied that electron transfer from the donor **TTF** to the acceptor fluorene backbone occurred in the ground state of **P2** (post).

As the addition of $\text{Fe}(\text{ClO}_4)_3$ to the solution of **P2** (post), the fluorescence intensity was recovered (Fig. 6). The oxidation of neutral **TTF** to the radical cation **TTF**^{•+} could prevent the **TTF**^{•+} from acting as an electron donor to quench the fluorescence of the fluorene units and resulted in fluorescence enhancement.⁶ In other words, when the pendant **TTF** units of **P2** (post) were oxidized chemically, the PET interaction between the **TTF** units and fluorene backbone would be hindered. Consequently, the fluorescence of **P2** (post) would be enhanced. This approach was proven to be a good method for the construction of new molecular switches.²⁹ Notably, compared with the molecular switches, the amplifying effect of the conjugated fluorescent polymers would be a great advantage.³⁰

Conductivity

The solutions of **P2** (post), **P3**, **P4** and **P5** in THF were treated with electron acceptor tetracyanoquinodimethane (TCNQ) and the doped films were obtained from a drop of cast solution of polymer/TCNQ (1 : 4 molar ratio) onto ITO glass plates,³¹ followed by drying in vacuum at 35 °C for 10 h. The conductivity of these polymers in the neutral and doped state was determined by four-probe conductivity measurements with a SX1934 apparatus and the values were shown in Table 2.

As shown in Table 2, the conductivity of **P2** (post) was at the lower potential in the neutral state and was increased

about 10^3 times after chemical doping with TCNQ, due to the oxidation of neutral **TTF** to **TTF**^{•+}. The acetylene linkages allowed the conjugated fluorene-based backbone to adopt a more planar structure and the increasing planarity and rigidity optimized the overlap of π -orbitals thus enhancing electron delocalization. In the doped state, the delocalized charges between the **TTF**^{•+} moiety and the conjugated fluorene-based backbone facilitated the π - π interactions between neighboring **TTF**^{•+} units^{10,32} and resulted in a considerable increase in conductivity. Meanwhile, the conductivity measurements performed on the doped **P3** and **P4**, also gave high values ($1\text{--}2 \times 10^{-3} \text{ S cm}^{-1}$). The results proved that doped **P2** (post), **P3** and **P4** were good candidates of organic conducting materials. Moreover, the doped polymers were stable in air and their conductivities were almost changeless just like other **TTF**-based polymers.¹⁰

Conclusions

We have developed two functionalization methods, *i.e.* prepolymerization and postpolymerization, to synthesize conjugated ethynylene-fluorene polymers with electro-donating **TTF** as pendant groups by using sonogashira coupling reaction. ¹H NMR showed that postpolymerization method would be a better approach for the highly functionalization effect. Meanwhile, this method could be of great utility, because it could be extended to synthesize other conjugated fluorene-based polymer bearing **TTF** units (**P3** and **P4**). The CV, UV-vis absorption spectra and fluorescence spectra showed there was photo-induced electron transfer (PET) interaction between **TTF** units and the ethynylene-fluorene backbone. The increasing amount (from 40% to 100%) of the **TTF** units in each repeat unit would enhance the effect. The chemical oxidation study implied that the fluorescence intensity of **P2** (post) could be modulated by the oxidation of **TTF** units. Moreover, the **TTF**-carrying conjugated fluorene-ethynylene polymers exhibited good solubility and higher conductivity (neutral conductivity around $2\text{--}4 \times 10^{-6} \text{ S cm}^{-1}$; doped conductivity around $1\text{--}3 \times 10^{-3} \text{ S cm}^{-1}$). These unique natures made them attractive candidates for fluorescence switches and conducting materials.

Experimental

Materials and instruments

All the reagents and solvents were of commercial quality and were distilled or dried when necessary using the standard procedures. ¹H NMR and ¹³C NMR spectra were obtained on Bruker AVANCE 400 instrument operating at 400 MHz and 100 MHz and chemical shifts were quoted downfield of

Table 2 The conductivity of neutral and doped **P2** (post), **P3**, **P4** and **P5**

Polymer	Neutral conductivity ^a /S cm ⁻¹	Doped Conductivity ^a /S cm ⁻¹
P2 (post)	3.6×10^{-6}	2.7×10^{-3}
P3	2.5×10^{-6}	1.3×10^{-3}
P4	3.1×10^{-6}	2.0×10^{-3}
P5	7.0×10^{-11}	9.0×10^{-11}

^a We tested five different positions for each film during conductivity measurements. The given data was the average value of these five data sets.

TMS. Elemental analyses were obtained from an Elemental vario EL III C, H, N analyzer. Mass spectra were recorded using LCQ ADVANTAGE mass spectrometer. Absorption spectra were measured with CARY 100 Conc UV-visible spectrophotometer. Fluorescence spectra were carried out with CARY Eclipse Fluorescence spectrophotometer and were corrected for the spectral response of the machines. Gel permeation chromatography (GPC) was carried out with Water-Breeze GPC apparatus using THF as eluent. All the electrochemical experiments were performed in CH_2Cl_2 with $n\text{-Bu}_4\text{NPF}_6$ as the supporting electrolyte, platinum as the working and counter electrodes, and saturated calomel electrode (SCE) as the reference electrode. The scan rate was 50 mV s^{-1} . The electric conductivity was measured using a four-probe technique with a SX1934 apparatus.

Syntheses

Monomer 2. To a solution of **TTF 1** (1.335 g, 2.35 mmol) in dried DMF (20 mL), $\text{CsOH}\cdot\text{H}_2\text{O}$ (0.42 g, 2.5 mmol) in absolute MeOH (6 mL) was added over a period of 30 min under nitrogen. After stirring for 1 h, a solution of **Monomer 1**^{33–35} (0.635 g, 1.175 mmol) in dried DMF (5 mL) was added dropwise over 30 min. The reaction mixture was stirred for another 12 h at room temperature. The solvent was removed under reduced pressure and the residue was purified by column chromatography on silica gel (CH_2Cl_2 : petroleum ether = 1:4) to give **Monomer 2** as dark-red oil (0.982 g, 59.3%). ^1H NMR (400 MHz, CDCl_3 , Me_4Si): δ 7.61 (d, 2H, $J = 8 \text{ Hz}$, ph-H), 7.47–7.43 (m, 4H, ph-H), 3.14 (s, 2H, $-\text{C}\equiv\text{CH}$), 2.80–2.70 (m, 8H, $-\text{S}-\text{CH}_2-$), 2.68–2.64 (m, 4H, $-\text{S}-\text{CH}_2-$), 2.33 (s, 6H, $-\text{S}-\text{CH}_3$), 1.94–1.91 (m, 4H, $-\text{CH}_2-$), 1.62–1.58 (m, 8H, $-\text{CH}_2-$), 1.38 (m, 12H, $-\text{CH}_2-$), 1.27 (m, 16H, $-\text{CH}_2-$), 1.11 (m, 4H, $-\text{CH}_2-$), 1.04–1.03 (m, 4H, $-\text{CH}_2-$), 0.86–0.85 (m, 12H, $-\text{CH}_3$), 0.54 (m, 4H, $-\text{CH}_2-$). ^{13}C NMR (100 MHz, CDCl_3 , Me_4Si): δ 150.70, 140.91, 131.37, 129.24, 127.76, 127.71, 126.43, 125.96, 121.01, 120.08, 110.52, 109.96, 84.42, 55.09, 40.11, 36.29, 36.10, 31.32, 29.73, 29.52, 29.41, 28.21, 28.07, 23.63, 22.56, 19.16, 14.10. MS (ESI, 25 eV): $m/z = 1408.3$ (M^+), 1431.2 ($\text{M}^+ + \text{Na}$). Found: C, 57.09; H, 6.41. Calcd. for $\text{C}_{67}\text{H}_{90}\text{S}_{16}$: C, 57.13; H, 6.44%.

Polymer P1. A mixture of compound **1** (540 mg, 1 mmol) and 4,4'-diiodobiphenyl (406 mg, 1 mmol) in diisopropylamine (8 mL) and toluene (16 mL) was degassed for 30 min. $\text{Pd}(\text{PPh}_3)_4$ (17.3 mg, 0.015 mmol) and CuI (8.6 mg, 0.045 mmol) were added. The mixture was stirred at r.t. for 48 h and then poured into methanol (200 mL) and filtrated. The solid was extracted with chloroform for 12 h using a Soxhlet apparatus. After removing most of the chloroform under reduced pressure, the concentration liquid was added to methanol (100 mL). The precipitate was filtrated and dried under vacuum at room temperature to give **polymer 1** as brown solid (511 mg, 73.8%). ^1H NMR (400 MHz, CDCl_3 , Me_4Si): δ 7.80–7.78 (m, 2H, ph-H), 7.70–7.64 (m, 6H, ph-H), 7.58–7.53 (m, 4H, ph-H), 7.37–7.36 (m, 2H, ph-H), 3.31–3.28 (m, 4H, $-\text{Br}-\text{CH}_2-$), 2.02 (m, 4H, $-\text{CH}_2-$), 1.69–1.66 (m, 4H, $-\text{CH}_2-$), 1.21–1.11 (m, 8H, $-\text{CH}_2-$), 0.64 (m, 4H, $-\text{CH}_2-$). GPC (THF, polystyrene standard): $M_n = 6036$, $M_w/M_n = 1.23$.

Polymer P2 (pre). The reaction procedure was similar to that of **monomer 2** using dried chloroform as the solvent. After the reaction finished, the reaction mixture was poured into methanol (200 mL) and filtrated. The solid was extracted with chloroform for 12 h using a Soxhlet apparatus. After removing most of the chloroform under reduced pressure, the concentration liquid was added to methanol (100 mL). The precipitate was filtrated and dried under vacuum at room temperature to give **P2 (pre)** as brown solid (0.328 g, 43.6%). ^1H NMR (400 MHz, CDCl_3 , Me_4Si): δ 7.73 (m, 2H, ph-H), 7.61–7.51 (m, 10H, ph-H), 7.33–7.32 (m, 2H, ph-H), 3.24 (m, 2H, $-\text{Br}-\text{CH}_2-$), 2.77–2.66 (m, 4H, $-\text{S}-\text{CH}_2-$), 2.41–2.31 (m, 2H, $-\text{S}-\text{CH}_3$), 1.98 (m, 2H, $-\text{CH}_2-$), 1.60 (m, 6H, $-\text{CH}_2-$), 1.37–1.07 (m, 22H, $-\text{CH}_2-$), 0.86 (m, 6H, $-\text{CH}_3$), 0.61 (m, 4H, $-\text{CH}_2-$). ^{13}C NMR (100 MHz, CDCl_3 , Me_4Si): δ 150.82, 140.73, 139.77, 139.73, 137.98, 132.15, 128.79, 127.74, 126.92, 126.79, 125.87, 122.04, 120.15, 110.58, 93.53, 91.39, 89.77, 55.18, 40.28, 36.29, 33.92, 32.67, 31.30, 29.70, 29.07, 28.20, 27.82, 23.59, 22.54, 19.14, 14.05. GPC (THF, polystyrene standard): $M_n = 6069$, $M_w/M_n = 1.16$.

Polymer P2 (post). A mixture of **monomer 2** (169 mg, 0.118 mmol) and 4,4'-diiodobiphenyl (48 mg, 0.118 mmol) in diisopropylamine (1 mL) and toluene (2 mL) was degassed for 30 min. $\text{Pd}(\text{PPh}_3)_4$ (2.7 mg, 0.002 mmol) and CuI (1.1 mg, 0.006 mmol) were added. The mixture was stirred at 70°C for 48 h and then poured into methanol (200 mL) and filtrated. The solid was extracted with chloroform for 12 h using a Soxhlet apparatus. After removing most of the chloroform under reduced pressure, the concentration liquid was added to methanol (100 mL). The precipitate was filtrated and dried under vacuum at room temperature to give **P2 (post)** as brown solid (0.148 g, 79.3%). ^1H NMR (400 MHz, CDCl_3 , Me_4Si): δ 7.81–7.79 (m, 1H, ph-H), 7.70–7.55 (m, 12H, ph-H), 7.39–7.37 (m, 1H, ph-H), 2.81–2.72 (m, 12H, $-\text{S}-\text{CH}_2-$), 2.37 (m, 6H, $-\text{S}-\text{CH}_3$), 2.03 (m, 4H, $-\text{CH}_2-$), 1.63 (m, 8H, $-\text{CH}_2-$), 1.40 (m, 12H, $-\text{CH}_2-$), 1.30 (m, 16H, $-\text{CH}_2-$), 1.21 (m, 4H, $-\text{CH}_2-$), 1.12–1.11 (m, 4H, $-\text{CH}_2-$), 0.89–0.88 (m, 12H, $-\text{CH}_3$), 0.65–0.64 (m, 4H, $-\text{CH}_2-$). ^{13}C NMR (100 MHz, CDCl_3 , Me_4Si): δ 150.93, 150.86, 139.68, 137.72, 132.41, 128.64, 127.66, 126.88, 126.74, 125.84, 122.01, 119.97, 110.34, 93.21, 91.49, 89.76, 55.18, 40.24, 36.29, 31.31, 29.62, 29.03, 28.22, 27.70, 23.50, 22.56, 19.15, 14.06. GPC (THF, polystyrene standard): $M_n = 13648$, $M_w/M_n = 1.24$.

Polymer P3. The procedure was similar to that of **P2 (post)** using 4,4'-diiodobiphenyl ether instead of 4,4'-diiodobiphenyl. **P3** was obtained as brown solid (0.196 g, 63.2%). ^1H NMR (400 MHz, CDCl_3 , Me_4Si): δ 7.61–7.48 (m, 10H, ph-H), 6.99–6.75 (m, 4H, ph-H), 2.75–2.65 (m, 12H, $-\text{S}-\text{CH}_2-$), 2.30 (m, 6H, $-\text{S}-\text{CH}_3$), 1.94 (m, 4H, $-\text{CH}_2-$), 1.56 (m, 8H, $-\text{CH}_2-$), 1.34–1.03 (m, 36H, $-\text{CH}_2-$), 0.83 (m, 12H, $-\text{CH}_3$), 0.56 (m, 4H, $-\text{CH}_2-$). ^{13}C NMR (100 MHz, CDCl_3 , Me_4Si): δ 156.55, 150.74, 140.57, 138.81, 133.28, 130.81, 129.23, 127.70, 125.95, 125.77, 122.04, 121.37, 120.04, 118.97, 110.57, 109.91, 90.01, 89.35, 86.78, 55.14, 40.25, 40.21, 40.19, 36.26, 36.10, 31.28, 29.69, 29.51, 29.42, 28.17, 28.07, 23.65, 22.52, 19.13, 14.05. GPC (THF, polystyrene standard): $M_n = 13481$, $M_w/M_n = 1.47$.

Polymer P4. The procedure was similar to that of **P2** (post) using 2,5-diiodoxylylene instead of 4,4'-diiodobiphenyl. **P4** was obtained as dark-brown solid (0.231 g, 76.0%). ¹HNMR (400 MHz, CDCl₃, Me₄Si): δ 7.70–7.65 (m, 4H, ph-H), 7.50–7.37 (m, 4H, ph-H), 2.78–2.68 (m, 12H, S–CH₂–), 2.52–2.34 (m, 12H, S–CH₃, ph-CH₃), 1.96 (m, 4H, –CH₂–), 1.60 (m, 8H, –CH₂–), 1.37–1.07 (m, 36H, –CH₂–), 0.86 (m, 12H, –CH₃), 0.58 (m, 4H, –CH₂–). ¹³CNMR (100 MHz, CDCl₃, Me₄Si): δ 151.00, 150.81, 139.66, 132.38, 129.32, 129.29, 127.76, 126.04, 126.01, 110.63, 109.98, 55.19, 40.21, 40.17, 36.36, 36.20, 31.30, 29.70, 29.51, 29.42, 28.20, 28.09, 27.37, 23.66, 22.54, 19.82, 19.29, 19.25, 14.06. GPC (THF, polystyrene standard): *Mn* = 6535, *Mw*/*Mn* = 2.08.

Acknowledgements

This work was supported by National Natural Science Foundation of China (No. 20676036, 20872035), Specialized Research Fund for the Doctoral Program of Higher Education (No. 20070251018).

References

- J. L. Segura and M. Martín, *Angew. Chem., Int. Ed.*, 2001, **40**, 1372–1409.
- M. R. Bryce, *J. Mater. Chem.*, 2000, **10**, 589–598.
- J. P. Farges, *Organic Conductors: Fundamentals and Applications*, ed. Marcel Dekker Publishers, New York, 1994, p. 1.
- G. X. Zhang, D. Q. Zhang, Y. C. Zhou and D. B. Zhu, *J. Org. Chem.*, 2006, **71**, 3970–3972.
- K. A. Nielsen, J. O. Jeppesen, E. Levillain and J. Becher, *Angew. Chem., Int. Ed.*, 2003, **42**, 187–191.
- H. C. Li, J. O. Jeppesen, E. Levillain and J. Becher, *Chem. Commun.*, 2003, **7**, 846–847.
- S. Inagi, K. Naka and Y. Chujo, *J. Mater. Chem.*, 2007, **17**, 4122–4135.
- M. Balog, H. Rayah, F. L. Derf and M. Sallé, *New J. Chem.*, 2008, **32**, 1183–1188.
- P. J. Skabara, D. M. Roberts, I. M. Serebryakov and C. Pozo-Gonzalo, *Chem. Commun.*, 2000, 1005–1006.
- Y. B. Liu, C. Y. Wang, M. J. Li, G. Q. Lai and Y. J. Shen, *Macromolecules*, 2008, **41**, 2045–2048.
- Y. B. Liu, C. Y. Wang, M. J. Li, G. Q. Lai and Y. J. Shen, *New J. Chem.*, 2008, **32**, 505–510.
- L. Huchet, S. Akoudad and J. Roncali, *Adv. Mater.*, 1998, **10**, 541–545.
- G. G. Abashev, E. V. Shklyayeva, R. V. Syutkin, K. Y. Lebedev, I. V. Osorgina, V. A. Romanova and A. Y. Bushueva, *Solid State Sci.*, 2008, **10**, 1710–1719.
- M. Fukuda, K. Sawada and K. Yoshino, *J. Polym. Sci., Part A: Polym. Chem.*, 1993, **31**, 2465–2471.
- H. P. Rathnayake, A. Cirpan, P. M. Lahti and F. E. Karasz, *Chem. Mater.*, 2006, **18**, 560–566.
- S. H. Lee, T. Nakamura and T. Tsutsui, *Org. Lett.*, 2001, **3**, 2005–2007.
- K. D. Belfield, K. J. Schafer, W. Mourad and B. A. J. Reinhardt, *J. Org. Chem.*, 2000, **65**, 4475–4481.
- X. C. Zhang, Y. Zhang, C. Y. Wang, G. Q. Lai, L. Zhang and Y. J. Shen, *Polym. Bull.*, 2009, **63**, 815–827.
- B. Liu, B. S. Gaylord, S. Wang and G. C. Bazan, *J. Am. Chem. Soc.*, 2003, **125**, 6705–6714.
- D. F. Perepichka, M. R. Bryce, E. J. L. McInnes and J. P. Zhao, *Org. Lett.*, 2001, **3**, 1431–1434.
- Y. H. Hou, X. J. Wan, M. Yang, Y. F. Ma, Y. Huang and Y. S. Chen, *Macromol. Rapid Commun.*, 2008, **29**, 719–723.
- Y. H. Hou, Y. S. Chen, Q. Liu, M. Yang, X. J. Wan, S. G. Yin and A. Yu, *Macromolecules*, 2008, **41**, 3114–3119.
- R. Chinchilla and C. Nájera, *Chem. Rev.*, 2007, **107**, 874–922.
- N. Svenstrup, K. M. Rasmussen, T. K. Hansen and J. Becher, *Synthesis*, 1994, **8**, 809–812.
- C. A. Christensen, M. R. Bryce and J. Becher, *Synthesis*, 2000, 1695–1704.
- E. J. Zhou, C. He, Z. A. Tan, C. H. Yang and Y. F. Li, *J. Polym. Sci., Part A: Polym. Chem.*, 2006, **44**, 4916–4922.
- J. Casado, R. P. Ortiz, M. C. Ruiz Delgado, V. Hernandez, J. T. López Nájarete, J. M. Raimundo, P. Blanchard, M. Allain and J. Roncali, *J. Phys. Chem. B*, 2005, **109**, 16616–16627.
- X. F. Guo, D. Q. Zhang, H. J. Zhang, Q. H. Fan, W. Xu, X. C. Ai, L. Z. Fan and D. B. Zhu, *Tetrahedron*, 2003, **59**, 4843–4850.
- C. Farren, C. A. Christensen, S. FitzGerald, M. R. Bryce and A. Beeby, *J. Org. Chem.*, 2002, **67**, 9130–9139.
- S. W. Thomas, G. D. Joly and T. M. Swager, *Chem. Rev.*, 2007, **107**, 1339–1386.
- P. J. Skabara, R. Berridge, E. J. McInnes, D. P. West, S. J. Coles, M. B. Hursthouse and K. Müllen, *J. Mater. Chem.*, 2004, **14**, 1964–1969.
- S. Frenzel, S. Arndt, R. Ma and K. Müllen, *J. Mater. Chem.*, 1995, **5**, 1529–1537.
- Y. Q. Huang, Q. L. Fan, S. B. Li, X. M. Lu, F. Cheng, G. W. Zhang, Y. Chen, L. H. Wang and W. Huang, *J. Polym. Sci., Part A: Polym. Chem.*, 2006, **44**, 5424–5437.
- Y. Q. Huang, Q. L. Fan, X. M. Lu, C. Fang, S. J. Liu, L. H. Yu-Wen, L. H. Wang and W. Huang, *J. Polym. Sci., Part A: Polym. Chem.*, 2006, **44**, 5778–5794.
- Y. Q. Huang, Q. L. Fan, G. W. Zhang, Y. Chen, X. M. Lu and W. Huang, *Polymer*, 2006, **47**, 5233–5238.